

# LIQUEFACTION POTENTIAL OF SANDS USING THE CPT

By Peter K. Robertson<sup>1</sup> and Richard G. Campanella,<sup>2</sup> M. ASCE

**ABSTRACT:** Existing methods for the evaluation of liquefaction potential using data obtained from the Cone Penetration Test (CPT) are reviewed. A modified CPT-based method for the liquefaction assessment of sand is presented. Information available on the liquefaction of silty sands is reviewed, and a procedure for considering the influence of silt content is also presented. Field and laboratory data from Canada, Japan, China and the United States are presented to provide a preliminary evaluation of the proposed CPT-based liquefaction assessment methods.

## INTRODUCTION

Some of the most comprehensive work on liquefaction and cyclic mobility assessment during earthquake loading was reported by Seed (20) and Seed, et al. (23).

In general, most methods available for evaluating the liquefaction or the cyclic mobility potential of a soil deposit subjected to earthquake loading involve two parts: (1) Estimation of the cyclic stress or strain condition developed in the field due to the design earthquake; and (2) estimation of the field liquefaction characteristics. For soil under level ground conditions, the cyclic characteristics are best represented by the average cyclic stress ratio,  $\tau/\sigma'_{vo}$ , i.e., the ratio of the average cyclic shear stress,  $\tau$ , developed on horizontal planes in the soil as a result of the earthquake motions to the initial vertical effective stress,  $\sigma'_{vo}$ . This parameter has the advantage of taking into account the depth of the soil layer involved, the depth of the water table and the intensity of earthquake or other cyclic loading phenomena (22).

Most methods compare the average cyclic stress ratio to cause liquefaction or a certain level of cyclic mobility,  $\tau_i/\sigma'_{vo}$ , with the average cyclic stress ratio generated by the earthquake ground motions,  $\tau/\sigma'_{vo}$ . By assuming undrained conditions, most methods ignore the possible effects of dissipation of excess pore pressures.

The cyclic stress ratios developed in the field due to earthquake loading can be computed using a simplified approach developed by Seed and Idriss (21).

The estimation of the field liquefaction characteristic is determined: (1) By use of field correlations using in-situ tests; or (2) by means of laboratory tests on representative samples of the soil deposit. Many problems exist in laboratory testing, e.g., adequate simulation of field con-

<sup>1</sup>NSERC Univ. Research Fellow, Univ. of British Columbia, Vancouver, British Columbia.

<sup>2</sup>Prof. and Head of Civ. Engrg. Dept., Univ. of British Columbia, Vancouver, British Columbia.

Note.—Discussion open until August 1, 1985. To extend the closing date one month, a written request must be filed with the ASCE Manager of Journals. The manuscript for this paper was submitted for review and possible publication on October 24, 1983. This paper is part of the *Journal of Geotechnical Engineering*, Vol. 111, No. 3, March, 1985. ©ASCE, ISSN 0733-9410/85/0003-0384/\$01.00. Paper No. 19552.

ditions, system compliance and membrane penetration and development of uniform shear stresses. Because of the difficulty in obtaining and testing undisturbed samples of cohesionless soils, many engineers prefer to adopt the field performance correlation approach (15).

Several field performance correlations have been developed using in-situ testing techniques as an index of field liquefaction characteristics. Examples of these are the Standard Penetration Test (12,23), the electrical resistivity probe (1) and the Cone Penetration Test (27). Other methods for the assessment of liquefaction potential have been developed using in-situ tests such as the self-boring pressuremeter (25) and the in-situ measurement of shear wave velocity (6), but these have not yet been fully correlated to field performance.

In general, there is very little field data available to establish good correlations of field performance with in-situ test methods other than the Standard Penetration Test (SPT). The SPT is the most commonly used in-situ test in North America and is conducted worldwide to a greater extent than any other in-situ soil test. However, despite continued efforts to standardize the SPT procedure, there are still continued problems associated with its repeatability and reliability.

The Cone Penetration Test (CPT), on the other hand, is becoming more popular as an in-situ test for site investigation and geotechnical design. The CPT is believed to be the most reliable tool for delineation of stratigraphy and the continuous rapid measurement of penetration resistance,  $q_c$ , and sleeve friction,  $f_s$ . The electric cone has also allowed the addition of pore-pressure measurements during penetration. The procedure and equipment of the quasi-static electric cone penetration test are easily standardized (24). The most significant advantages of the CPT are its simplicity, repeatability, accuracy and continuous record. Because of the inherent variability of most soil deposits, the continuous nature of CPT data is extremely valuable.

This paper outlines alternate ways in which the CPT can and has been correlated to liquefaction resistance, and presents limited field and laboratory data to evaluate the correlations. The applicability and potential of continuous pore-pressure measurements during cone penetration are also briefly discussed.

## EXISTING CPT-BASED LIQUEFACTION ASSESSMENT METHODS

Liquefaction studies in China have led to a correlation between earthquake shaking conditions causing liquefaction or cyclic mobility and the cone penetration resistance of sands (27). In this correlation, the critical value of cone penetration resistance,  $q_{crit}$ , separating liquefiable from nonliquefiable conditions to a depth of 15 m, is determined by

$$q_{crit} = q_{w0}[1 - 0.065(H_w - 2)][1 - 0.05(H_0 - 2)] \dots \dots \dots (1)$$

in which  $H_w$  = depth of water level below ground surface in meters;  $H_0$  = depth to top of sand layer under consideration; and  $q_{w0}$  = function of the shaking intensity as shown in Table 1. This empirical equation was the result of field test data from the Tangshan earthquake area, where the sand was primarily a clean sand with little fine content. The mean grain size was  $D_{50} = 0.25$  mm. The method was later expanded (28) to

**TABLE 1.—Shaking Intensity**

Maximum surface acceleration, $a_{max}$ (1)	Reduced epicentral distance, in kilometers (2)	Critical penetration resistance $q_c$ , in kilograms per square centimeters (3)	Modified mercalli intensity (4)
0.1 g	80.5	47	VII
0.2 g	38.0	117	VIII
0.4 g	18.6	180	IX

Note: Chinese Code.

incorporate data from a silty sand site (Lutai), where  $D_{50} = 0.07$  mm. The practical application of this method may present some difficulty since the epicentral distance and intensity of shaking is involved.

Another method that uses cone penetration resistance for the assessment of liquefaction potential was developed by Douglas, et al., (9). This method involves the conversion of CPT data to equivalent SPT  $N$  values by conducting preliminary studies at each new site to establish the correlation between  $q_c$  and  $N$  for the particular sand at the site. The equivalent SPT  $N$  values can then be used in SPT-based liquefaction resistance correlations.

Seed, et al. (23), recently proposed a correlation between liquefaction resistance for level ground conditions and CPT data. The method uses the available correlations (19) between SPT and CPT test data, and applies them to the critical boundaries separating liquefiable from nonliquefiable conditions using the extensive database of the SPT correlation with field liquefaction characteristics. A summary of the Seed, et al. (23), CPT method is shown in Fig. 1. The range between the proposed curves, however, is very large, especially at the larger penetration resistance values.

**DEVELOPMENT OF MODIFIED CPT BASED LIQUEFACTION ASSESSMENT METHODS**

The penetration resistance of both the SPT and CPT and the resistance of soil to liquefaction are similarly influenced by most soil compositional and environmental variables (19). These variables include soil density, soil structure, cementation, aging, stress state and stress history. Thus a knowledge of how these variables influence the resistance to cone penetration can be applied to provide a correlation between CPT resistance and liquefaction resistance.

**Normalized Cone Resistance.**—Since the SPT method proposed by Seed and Idriss (21) has proven extremely successful, it would appear logical to produce a CPT method along similar lines. Thus, one of the first requirements would be to modify the cone bearing,  $q_c$ , to an overburden stress level of 1 kg/cm<sup>2</sup> (1 tsf) or 100 kPa, using the relation:

Modified Cone Penetration Resistance,  $Q_c = C_Q \cdot q_c$  ..... (2)

Since most calibration chamber test studies show that the cone bearing,

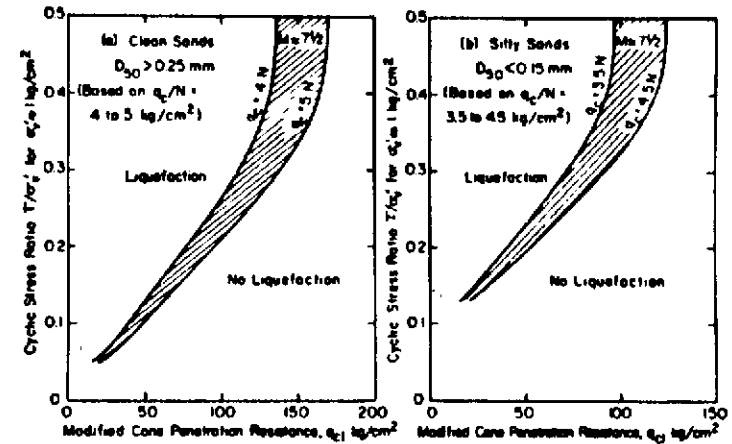


**FIG. 1.—Correlation Between Liquefaction Resistance of Sands for Level Ground Conditions and Modified Cone Penetration Resistance (After Seed, et al., Ref. 23)**

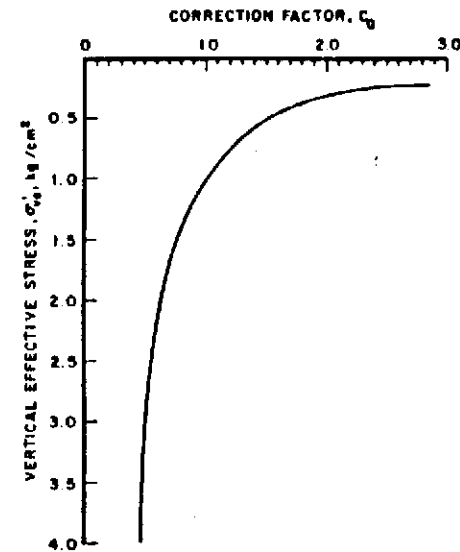
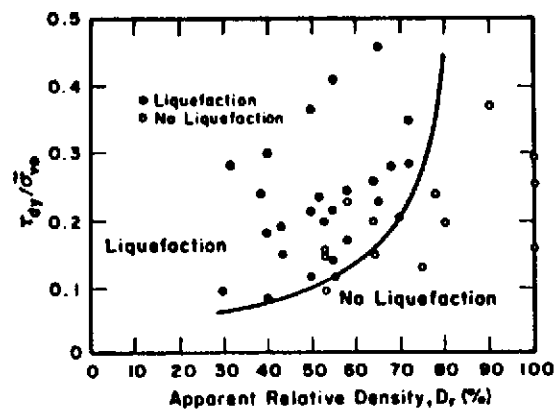


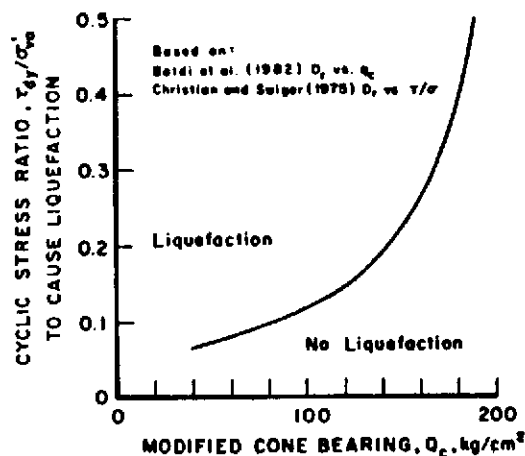
**FIG. 2.—Proposed Variation of Correction Factor,  $C_Q$ , with Effective Overburden Pressure**

$q_c$ , versus relative density ( $D_r$ ) relationships all have similar shapes (16), it should be possible to modify  $q_c$  using one of these correlations. The writers have carried this out using the very comprehensive data produced by Baldi, et al. (2), and the resulting correction factors are shown in Fig. 2. The correction factors,  $C_Q$ , shown in Fig. 2 are very similar to those proposed by Schmertman (18) and to the factor  $C_N$  proposed by Seed, et al. (23) for the SPT. This illustrates that CPT and SPT resistances



Based on Data by Christian and Swiger, 1975

FIG. 3.—Analysis of Field Records of Sites Where Liquefaction Did and Did Not Occur (After Vaid, et al., Ref. 25)

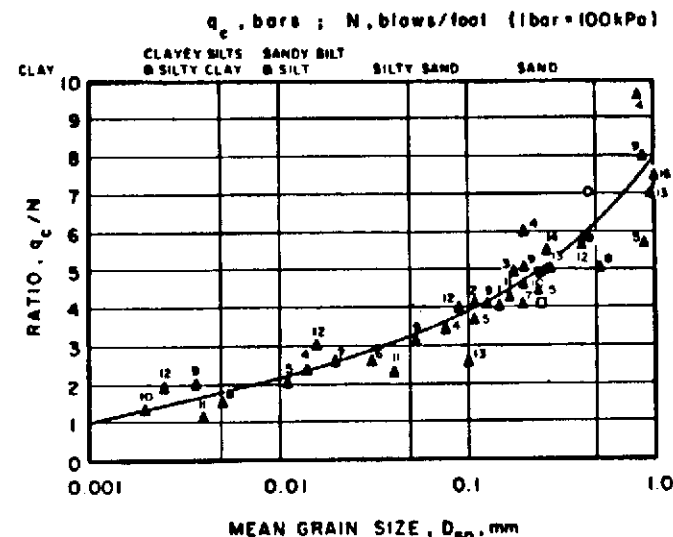


Based on:  
Baldi et al. (1982)  $Q_c$  vs.  $q_c$   
Christian and Swiger (1975)  $Q_c$  vs.  $\tau/\sigma'$

FIG. 4.—Correlation Between Liquefaction Resistance and Modified Cone Penetration Resistance for Sands Based on Relative Density Correlation

vary in a similar manner with depth for sand at a constant relative density.

**Relative Density Correlation.**—As a first step in a CPT method for liquefaction assessment, use can be made of the relative density correlation by Baldi, et al. (3). This has been done by the writers by combining the field liquefaction resistance data produced by Christian and Swiger (5) (Fig. 3) to produce the CPT resistance curve shown in Fig. 4. The liquefaction resistance curve by Christian and Swiger (5) has been chosen because it appears to represent quite closely the observed field liquefaction behavior.



- |                                |                                  |
|--------------------------------|----------------------------------|
| 1. Meyerhof (1956)             | 9. Nixon (1982)                  |
| 2. Meigh and Nixon (1961)      | 10. Krulzinga (1982)             |
| 3. Rodin (1961)                | 11. Douglas (1962)               |
| 4. De Alencar Veloso (1959)    | 12. Muromachi & Kobayashi (1982) |
| 5. Schmertmann (1970)          | 13. Goel (1982)                  |
| 6. Sutherland (1974)           | 14. Ishihara & Koga (1981)       |
| 7. Thornburn & MacVicar (1974) | 15. Leung (1983)                 |
| 8. Campanella et al. (1979)    | 16. Mitchell (1983)              |

TILBURY ISLAND SITE { □ SPT  $N_c$ ,  $ER_1 = 47\%$       ○ SPT  $N_c$ ,  $ER_1 = 65\%$   
 { ■ SPT  $N_c$ ,  $ER_1 = 55\%$       ● SPT  $N_c$ ,  $ER_1 = 55\%$  } UBC SITE, see Diagram Form

FIG. 5.—Variation of  $q_c/N$  Ratio with Mean Grain Size (After Robertson, et al., Ref. 17)

**SPT-CPT Correlation.**—Possibly a more logical method to derive a CPT liquefaction relation is by conversion of SPT to CPT. This has several advantages: The SPT liquefaction method is based on a large amount of experience from observed cases of liquefaction (23) and the SPT and CPT are both similarly influenced by most soil variables. Thus, correct conversion of SPT data to CPT can better account for factors, such as aging and stress history, that the density relationship cannot.

A considerable number of studies (see Fig. 5) have taken place over the years to quantify the relationship between SPT  $N$  values and CPT tip resistance,  $q_c$ . A wide range of  $q_c/N$  ratios have been published leading to much confusion. The variation in the published  $q_c/N$  ratio can be rationalized somewhat by reviewing the derived  $q_c/N$  ratios as a function of mean grain size ( $D_{50}$ ). A summary of many of the derived  $q_c/N$  relationships is shown in Fig. 5, as a function of mean grain size ( $D_{50}$ ).

It is clear that the  $q_c/N$  ratio increases with increasing grain size. The scatter in results appears to increase with increasing grain size. This is not surprising, since penetration in gravelly sand ( $D_{50} \approx 1.0$  mm) is significantly influenced by the larger individual gravel-sized particles, not to mention the variability of delivered energy in the SPT data. Also, sand deposits in general are usually stratified or nonhomogeneous, causing rapid variations in SPT  $N$ -values and CPT tip resistance. There was also some difficulty in defining the  $D_{50}$  from some of the references.

The  $q_c/N$  relation is significantly affected by SPT hammer type, since this affects the energy transmitted to the rods.

A recent publication (17) examined how the  $q_c/N$  ratio varies with the amount of energy delivered to the drill rods. Kovacs, et al. (14), and Robertson, et al. (17), have shown that the energy delivered to the rods during a SPT can vary from about 20–90% of the theoretical maximum, 475 J (4,200 in.-lb). The energy delivered to the drill stem varies with the number of turns of rope around the cathead, and varies with the fall height, drill rig type, hammer and anvil type, and operator characteristics.

When using the rope and cathead procedure with two turns of the rope, the typical energy delivered from standard donut- and safety-type hammers is about 50–60% of the theoretical maximum (13). Schmertmann (18) has suggested that, based on limited data, an efficiency of about 55% may be the norm for which it can be assumed that many North American SPT correlations were developed. Most of the data presented in Fig. 5 were obtained using standard donut-type hammers with a rope and cathead system.

Robertson, et al. (17), presented energy measurements on SPT data that indicate that the average energy ratio of 55% may represent the average energy level associated with the  $q_c/N$  correlation shown in Fig. 5.

The SPT liquefaction method by Seed was based on data mainly obtained using standard donut- and safety-type hammers with two turns of the rope around the drum (cathead). The work by Kovacs, et al. (14), would indicate that the average efficiency of the energy delivered to the rods using the foregoing (Seed) procedure ranges from 50–60%. Thus, the correlation shown in Fig. 5 can be used to convert CPT data to equivalent SPT  $N$  values for use in the Seed SPT-based liquefaction correlations. For medium sands ( $D_{50} = 0.25$  mm), a  $q_c/N$  ratio of 4.5–5.0 can therefore be considered representative.

For silty soils ( $D_{50} = 0.1$  mm), a  $q_c/N$  ratio of 4.0 can be considered more representative. As mentioned earlier, the SPT and CPT are similarly influenced by most soil variables and thus  $N$  and  $q_c$  appear to vary similarly with depth (i.e.,  $\sigma'_{vo}$ ). Thus, the  $q_c/N$  ratio can be used to directly convert normalized  $N_1$  to  $Q_c$  values, with little error.

The recent SPT and liquefaction data studied by Seed, et al. (23), show several data points where liquefaction did occur that plot below the original dividing line. A proposed lower bound to the SPT data points is shown in Fig. 6. The resulting lower bound appears to agree better with the field data shown in Fig. 3.

**Proposed CPT Liquefaction Relationship.**—A comparison between the different CPT liquefaction relations suggested here is shown in Fig. 7.

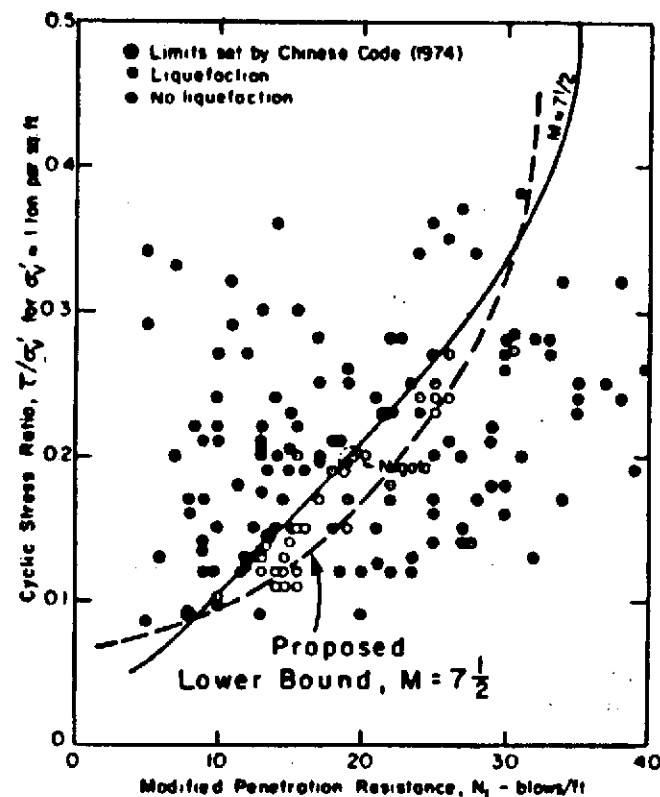


FIG. 6.—Correlation Between Liquefaction Resistance and SPT Showing Proposed Lower Bound (Data from Seed, et al. Ref. 23)

The relative density ( $D_r$ ) curve was obtained from Fig. 4. The SPT curve was obtained using the lower bound correlation proposed in Fig. 6 with a  $q_c/N$  ratio of 4.5, as suggested from Fig. 5. A proposed CPT design correlation was chosen on the bases of the following:

1. Factors such as aging, cementation and stress history tend to increase the resistance to liquefaction. Therefore, a relationship based on relative density ( $D_r$ ), such as that shown in Fig. 4, may tend to underestimate the liquefaction resistance; thus, the proposed design correlation is larger than the  $D_r$  curve.

2. The SPT correlation is based on a large amount of field observations which include factors such as aging, cementation and stress history. Thus, the relation based on SPT data will tend to be more representative of field behavior. However, the  $q_c/N$  ratio of 4.5 is an average low value for sands ( $D_{50} \geq 0.25$  mm) based on a standard 2 rope-turn-around-the-cathead hammer energy level. Some of the data, reviewed by Seed and Idriss (22), particularly the Japanese data, was almost certainly obtained using higher energy hammers where  $q_c/N$  ratios may be closer to 5.5

(10). Also, for medium to coarse sand ( $D_{50} > 0.25$  mm) the ratio will tend towards 5.5. Thus, the proposed design correlation is lower than the SPT ( $q_c/N = 4.5$ ) curve.

The proposed CPT design correlation shown in Fig. 7 is therefore based

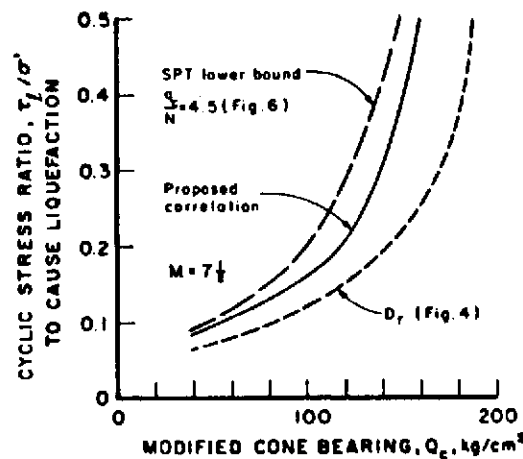


FIG. 7.—Summary of Correlations Between Liquefaction Resistance and Modified Cone Penetration Resistance in Sands

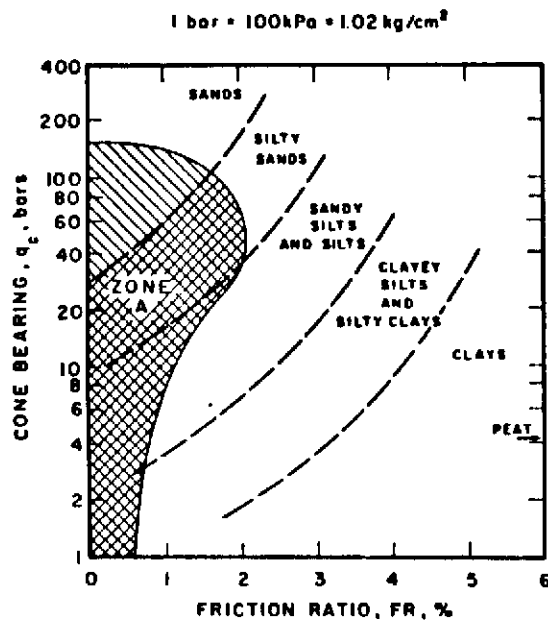


FIG. 8.—Soil Classification Chart for Electric Cone Showing Proposed Zone of Liquefiable Soils

predominantly on field observations of liquefaction-related phenomena for earthquakes of magnitude 7.5 (see Figs. 3 and 6). The correlation can be extended to earthquakes of different magnitudes, as suggested by Seed, et al. (23).

**Silty Sands.**—The proposed correlation shown in Fig. 7, however, is only applicable to clean sands with  $D_{50} \geq 0.25$  mm. To identify sands of this nature with CPT data alone, use can be made of the soil classification chart developed by Douglas and Olsen (8) but adapted by the writers, as shown in Fig. 8. Work by Douglas (7) and experience gained at the University of British Columbia (UBC) would suggest that soils susceptible to liquefaction fall within an area on the soil classification chart designated Zone A. Loose clean quartz sands with a  $D_{50} \geq 0.25$  mm tend to fall within the upper area of Zone A with  $30 \text{ kg/cm}^2 < q_c < 150 \text{ kg/cm}^2$  and friction ratio,  $FR < 1.0$ . Soils that fall within the lower area of Zone A are the loose silty sands and silts, since a decrease in mean grain size tends to cause a decrease in penetration resistance. These soils tend to have higher resistance to liquefaction for the same penetration resistance values and tend to develop more pore pressures during penetration because of their lower permeability.

Field and laboratory observations have shown that the liquefaction resistance tends to increase with decreasing grain size below a mean grain size ( $D_{50}$ ) of approximately 0.25 mm. It appears, however, that this increase is also associated with an increase in the cohesive nature of the soil. This effect was incorporated into the SPT-based method proposed by Iwasaki, et al. (12), by increasing the cyclic stress ratio to cause liquefaction by an amount dependent on the mean grain size, using the relation

$$\frac{\Delta\tau}{\sigma'_{vo}} = -0.146 \log \cdot \frac{D_{50}}{0.35} \text{ (mm)} \dots\dots\dots (3)$$

This was based on laboratory results and shows that there is a steady gradual increase in liquefaction resistance with decreasing grain size below a mean grain size of  $D_{50} = 0.6$  mm. The field data reviewed by Seed, et al. (23), showed an increase in cyclic stress ratio of about 0.075 with a decrease in mean grain size ( $D_{50}$ ) from 0.25–0.15 mm. This corresponds to a decrease in the SPT  $N$  value of about 7.5 for a constant cyclic stress ratio. For comparison, the Iwasaki, et al. (12), method predicts a 0.04 increase with a decrease in mean grain size from 0.25–0.15 mm. Data from Chinese CPT work (28) in silty sands indicate a decrease in cone resistance of about  $40 \text{ kg/cm}^2$  for a decrease in grain size from a medium sand ( $D_{50} \approx 0.25$  mm) to a silty sand ( $D_{50} \approx 0.15$  mm). This is equivalent to an increase in cyclic stress ratio to cause liquefaction of about 0.05 for constant cone resistance. The writers have combined these observed responses to generate a second correlation for CPT-based liquefaction by decreasing the proposed sand correlation shown in Fig. 7 by a cone resistance of  $40 \text{ kg/cm}^2$ . The combined proposed CPT-based liquefaction correlations are shown in Fig. 9.

The correlations proposed in Fig. 9 for CPT data are based on empirical relationships and require considerable field verification. The CPT-based method should be used in the same manner proposed by Seed, et al. (23), for the SPT-based method. The CPT data can be used to pro-

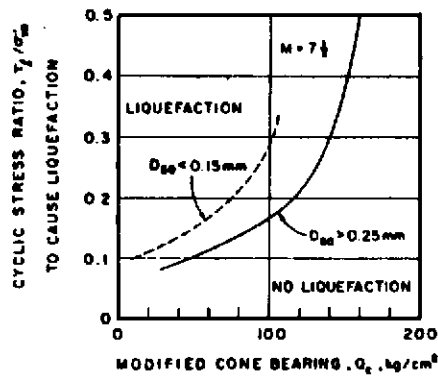


FIG. 9.—Proposed Correlations Between Liquefaction Resistance under Level Ground Conditions and Modified Cone Penetration Resistance for Sands and Silty Sands

vide a preliminary identification of liquefaction-susceptible soils using the chart shown in Fig. 8. Soils that fall within the upper shaded area of Zone A can be considered as sands with a  $D_{50} \geq 0.25$  mm. Soils that fall within the lower hatched area of Zone A can be considered as silty sands or silts with a  $D_{50} \leq 0.15$  mm. The CPT data would provide a continuous and repeatable measure of the penetration resistance and the correlations in Figs. 8 and 9 can be expected to provide a preliminary estimate of liquefaction potential. The CPT would provide data to identify potential critical areas where detailed assessment may be required, which may include sampling or further in-situ testing, or both.

#### PRELIMINARY EVALUATION OF PROPOSED CPT CORRELATION

To evaluate the proposed CPT liquefaction assessment curve shown in Fig. 9, data obtained from the literature has been reviewed by the writers from a number of sites around the world. The data will be presented in the following sections.

A summary of field and laboratory data from three sites are presented in Table 2. The sites are described in detail, and include Vancouver, B.C., Canada (Campanella et al., Ref. 5); Niigata, Japan (Ishihara and Koga, Ref. 11; and Tokyo Bay, Japan (Ishihara, et al., Ref. 12).

The data includes field CPT and SPT penetration resistance profiles and laboratory cyclic triaxial results carried out on undisturbed samples obtained from boreholes adjacent to the CPT and SPT soundings. The values of the laboratory-derived cyclic stress ratio to produce liquefaction or 10% double amplitude strain in 15 cycles have been plotted against modified cone resistance,  $Q_c$ , and compared to the proposed CPT liquefaction curves in Fig. 10.

The data from Canada and from Niigata, Japan, for sands with  $D_{50} > 0.25$  mm, plot close to the proposed sand resistance curve. The data from Canada and Tokyo Bay, Japan, for silty sands with  $D_{50} < 0.15$  mm plot close to or above the proposed silty sand resistance curve. It is in-

TABLE 2.—Summary of Field and Laboratory Results from Vancouver, Canada; Niigata and Tokyo Bay, Japan

Site (1)	Sample number (2)	Depth, in meters (3)	Verti- cal effec- tive stress, $\sigma'_{vm}$ , in kilo- grams per square centi- meter (4)	$D_{50}$ , in milli- meters (5)	Rela- tive den- sity, $D_r$ , as a per- centage (6)	Cone Resistance		SPT		Cyclic Stress Ratio to Cause 10 Percent Strain in 15 Cycles	
						$q_c$ , in kilo- grams per square centi- meter (7)	$Q_c$ , in kilo- grams per square centi- meter (8)	N (9)	$N_1$ (10)	$\sigma_d/\sigma'_m$ (11)	$\tau/\sigma'_m$ <sup>d</sup> (12)
Vancouver, Canada (Mc- Donald's Farm site)	1	3.5	0.40	0.45	45	40	70	3	5	0.20	0.13
	2	4.8	0.53	0.15	41	30	45	6	8	0.25	0.16
	3	6.3	0.68	0.50	59	80 <sup>a</sup>	104	12 <sup>b</sup>	15	0.33	0.21
	4	9.4	1.00	0.60	68	120	120	18 <sup>b</sup>	18	0.34	0.22
	5	10.9	1.14	0.30	13 <sup>c</sup>	105 <sup>a</sup>	95	20 <sup>b</sup>	19	0.32	0.21
	6	12.4	1.29	0.50	51	160 <sup>a</sup>	136	17 <sup>b</sup>	14	0.35	0.23
	7	14.0	1.43	0.12	50	50 <sup>a</sup>	40	11 <sup>b</sup>	8.5	0.30	0.20
Niigata, Japan (Kawa- gishi-cho site)	S1	2.45	0.45	0.32	56	20	33	3	4.5	0.20	0.13
	S2	5.45	0.75	0.42	54	42	51	8	9.5	0.18	0.12
	S3	6.95	0.90	0.35	50	67	72	10	10.5	0.17	0.11
	S4	8.45	1.05	0.24	64	60	58	12	12	0.21	0.14
	S5	9.45	1.15	0.35	52	50	45	13	12	0.21	0.14
	S6	11.45	1.35	0.26	55	54	46	21 <sup>a</sup>	17.5	0.18	0.12
	S8	13.45	1.55	0.25	53	70 <sup>a</sup>	53	10	8.5	0.18	0.12
	S9	14.45	1.65	0.28	79	90	65	14 <sup>a</sup>	11.5	0.25	0.16
	01	2.4	0.44	0.39	50	20	33	3	4.5	0.20	0.13
	02	5.4	0.74	0.42	53	42	51	8	9.5	0.20	0.13
03	6.4	0.84	0.47	66	60 <sup>a</sup>	67	9	9.5	0.25	0.15	
04	8.4	1.04	0.28	50	60	58	12	12	0.25	0.16	
05	10.4	1.24	0.52	47	35	31	14	12.5	0.18	0.12	
06	12.4	1.44	0.35	50	50 <sup>a</sup>	40	11	9	0.21	0.14	
07	14.4	1.64	0.28	55	90	65	14 <sup>a</sup>	11.5	0.23	0.15	
Niigata, Japan (Show Bridge, South Bank Site)	S1	4.45	0.50	0.28	70	50 <sup>a</sup>	75	18 <sup>a</sup>	25	0.26	0.16
	01	4.6	0.52	0.29	83	90 <sup>a</sup>	133	20 <sup>a</sup>	28	>0.36	>0.23
	02	4.9	0.55	0.29	85	125 <sup>a</sup>	180	30 <sup>a</sup>	42	>0.36	>0.23
Tokyo Bay, Japan (Owl Island No. 1)	03	5.2	0.58	0.29	87	160 <sup>a</sup>	225	35 <sup>a</sup>	47	>0.36	>0.20
	1	4.9	0.54	0.1	—	15	22	9	13	0.36	0.25
	2	5.9	0.63	0.15	—	25	35	5	7	0.40	0.26
	3	6.7	0.70	0.15	—	25	33	5	7	0.25	0.16
	4	8.4	0.86	0.03	—	6	7	3	3	0.40	0.26
5	13.9	1.85	0.15	—	11	9.5	6	5	0.33	0.22	

<sup>a</sup>Penetration resistance varies over sample length—average value estimated.

<sup>b</sup>Interpolated value from SPT profile.

<sup>c</sup>Some wood in sample  $D_r$ , not reliable.

<sup>d</sup> $\tau/\sigma'_m = c(\sigma_d/2\sigma'_m)$ , in which  $c$ , is taken to be 0.65.

teresting to note that much of the silty sand data plots well above the proposed CPT correlation.

Tangshan, China.—As mentioned earlier, Zhou (27) performed cone penetration tests in the Tangshan area of China and obtained an empirical correlation between cone penetration resistance and earthquake intensity. In his correlation, the critical value of cone penetration resis-

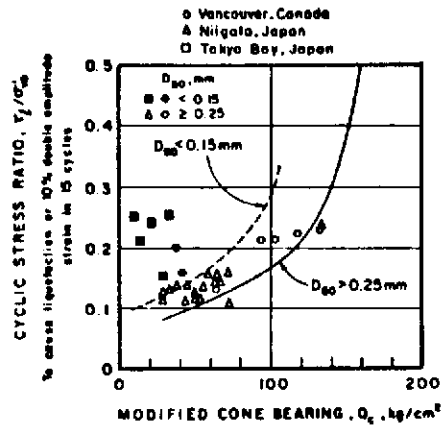


FIG. 10.—Correlation Between Laboratory Cyclic Stress Ratio and Modified Cone Penetration Resistance at Niigata and Tokyo Bay, Japan, and Vancouver, Canada

tance,  $q_{crit}$ , separating liquefiable from nonliquefiable conditions to a depth of 15 m, was defined.

This correlation can be reduced to the same parameters as those in Fig. 9, with the aid of correlations between earthquake shaking intensity and maximum ground accelerations. Unfortunately, there is no unique correlation between intensity and maximum ground acceleration. However, the Chinese code (27) suggests maximum surface accelerations for

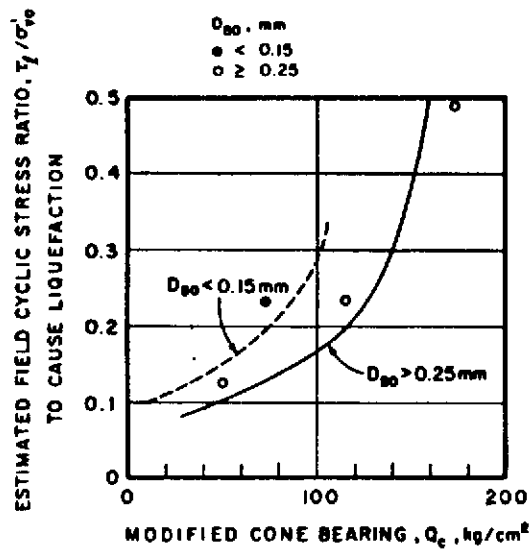


FIG. 11.—Correlation Between Estimated Field Cyclic Stress Ratio and Modified Cone Penetration Resistance at Tangshan, China (Data from Zhou, Refs. 27 and 28)

different earthquake intensities, and since the CPT correlation is based on Chinese data, it appears logical to use the Chinese code correlation. If the maximum surface accelerations are used to estimate the field cyclic stress ratio, the data obtained by Zhou (27) will result in the points shown in Fig. 11. Remarkably good agreement is obtained between the proposed CPT correlation and the independently obtained Chinese data. The usefulness of the Chinese data is that it is based entirely on field performance.

Zhou (28) expanded the database using data from a silty sand site (Lutai) where  $D_{50} = 0.07$  mm. This additional data point is included in Fig. 11 and agrees with the proposed silty sand resistance line.

The electric cone used by Zhou does not conform to European or American standards. The cone was 16 cm<sup>2</sup>, and had a 60° tip with a 100 cm<sup>2</sup> friction sleeve immediately behind the tip. The diameter reduced to the smaller diameter push rods immediately behind the friction sleeve. The standard cone has a 10 cm<sup>2</sup> base area, a 60° cone and a 150 cm<sup>2</sup> friction sleeve. However, based on Schmertmann's work with the mechanical cone, which also reduces in diameter behind the tip, the cone resistance values from the Chinese cone can be expected to be similar to those obtained with a standard electric cone.

Imperial Valley, U.S.A.—Youd and Bennett (26) presented some CPT data from two sites in the Imperial Valley, California, which experienced some liquefaction effects during the 1979 earthquake. Full details of the

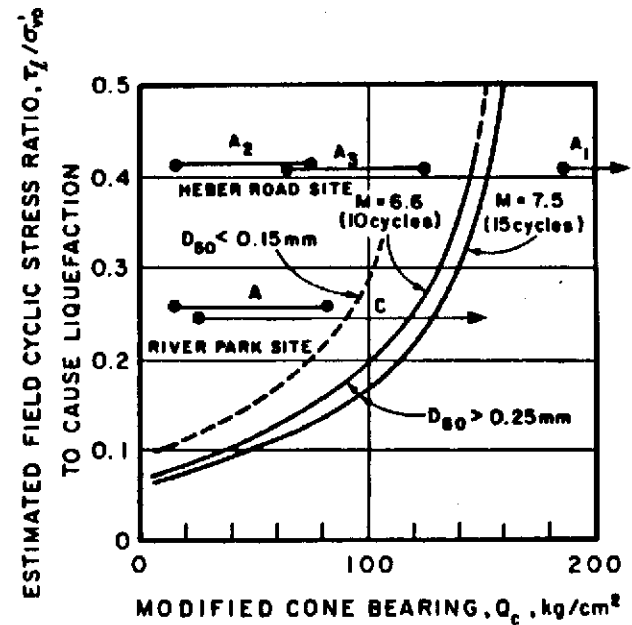


FIG. 12.—Correlation Between Estimated Field Cyclic Stress Ratio and Modified Cone Resistance in 1979, Imperial Valley Earthquake, California (Data from Youd and Bennett, Ref. 26)

sites are given by Youd and Bennett (26).

One site was located on Heber Road, where lateral spreading disrupted the pavement about 1 km northeast of the Imperial Fault. Youd and Bennett (26) identified three major sand deposits underlying the site. One sand deposit (Unit A<sub>2</sub>) was considered by Youd and Bennett to have liquefied, and another sand deposit (Unit A<sub>3</sub>) was considered to have developed high pore pressures and limited shear-strain (cyclic mobility). A third sand deposit (Unit A<sub>1</sub>) was not considered to have liq-

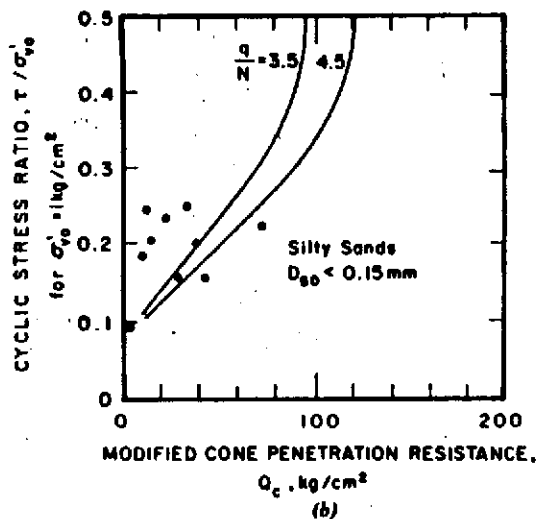
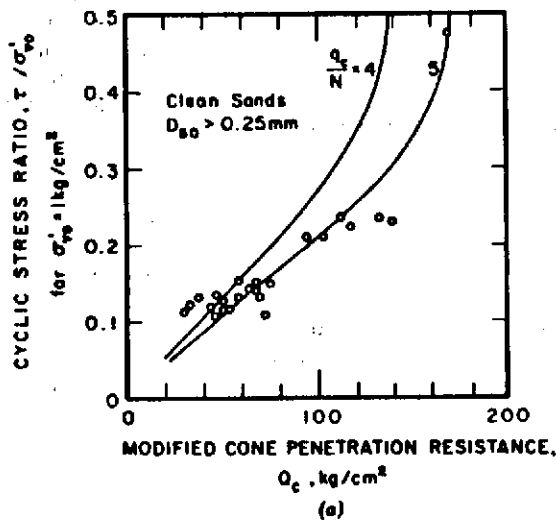


FIG. 13.—(a) Comparison of CPT Liquefaction Data for Clean Sands with Seed, et al. (23), CPT Correlation; (b) Comparison of CPT Liquefaction Data for Silty Sands and Silts with Seed, et al. (23), CPT Correlation

uefied. The range of modified cone resistance values from the three sand deposits is shown in Fig. 12. The Imperial Valley earthquake in 1979 was of magnitude 6.6. The corresponding CPT resistance curve for a  $M = 6.6$  earthquake (i.e., 10 cycles at  $0.65 \tau_{max}$ ) is shown in Fig. 12. The estimated field cyclic stress ratio at Heber Road was thought to be about 0.4 (Youd, personal communication, 1984). Fig. 12 indicates that Unit A<sub>2</sub> is highly susceptible to liquefaction, since it lies well above the resistance curve; Unit A<sub>3</sub> is also susceptible to liquefaction but would have limited shear-strain potential; and Unit A<sub>1</sub> is resistant to liquefaction. The field evidence supports these predictions.

The other site studied by Youd and Bennett (26) was located at River Park. The River Park site had a layer of brown flood-plain sediment, 1.8–2.5 mm thick (Unit A) at ground surface. The flood-plain sediment ranged from a sandy silt to silt to clayey silt. The silty layer overlies a 0.9–1.5 m thick layer of soft-to-medium-stiff flood-basin clay (Unit B). A massive bed of gray point-bar sand (Unit C) underlies the clay layer. The sand immediately beneath the clay ranges from loose to moderately dense. The density increases with depth so that within a few feet below the base of the clay the sand has a cone resistance greater than 100 kg/cm<sup>2</sup> and SPT  $N$  value greater than 20. During the 1979 earthquake, sand boils containing both types of sand (Unit A and C) erupted at River Park. The range of modified cone resistance values from the two sand deposits at the River Park site are shown in Fig. 12. CPT results indicate that the silty sand surface layer (Unit A) is susceptible to liquefaction and that the upper few feet of the underlying sand (Unit C) is also susceptible to liquefaction. The field evidence support these predictions.

**Summary.**—Considering the fact that all the data presented here were obtained from many independent sources, the agreement is very promising. The sand curve ( $D_{50} > 0.25$  mm) appears to represent a good lower bound to the available data. The silty sand curve ( $D_{50} < 0.15$  mm) also represents a good lower bound, but several laboratory-derived points plot considerably higher than the lower bound line. This highlights the insensitive nature of penetration resistance as a measure of liquefaction or cyclic mobility resistance in fine-grained soils. However, cone penetration in these fine-grained soils often takes place under undrained conditions and dynamic pore pressures can be generated.

As a comparison, the same CPT data shown in Figs. 10 and 11 are presented in relation to the CPT correlation proposed by Seed, et al. (23), and are shown in Figs. 13(a) and 13(b). Several of the data points in Fig. 13 plot below the Seed, et al. (23), correlations. This would indicate that the larger  $q_c/N$  ratio values of 5 and 4.5, suggested by Seed, et al. (23), are more applicable for the sand and silty sand correlations, respectively. Even so, these values may still produce slightly unconservative liquefaction resistance values.

One of the major advantages of CPT data for the evaluation of liquefaction potential in sands is the continuous nature of the results. This is illustrated in Fig. 14 which shows a comparison of predicted cyclic stress ratio to cause liquefaction at the Vancouver site. Fig. 14 compares the predicted cyclic stress ratio to cause liquefaction from SPT, CPT (using Fig. 9) and laboratory testing. Both the SPT and CPT methods agree remarkably well with the laboratory-measured values. The CPT method,

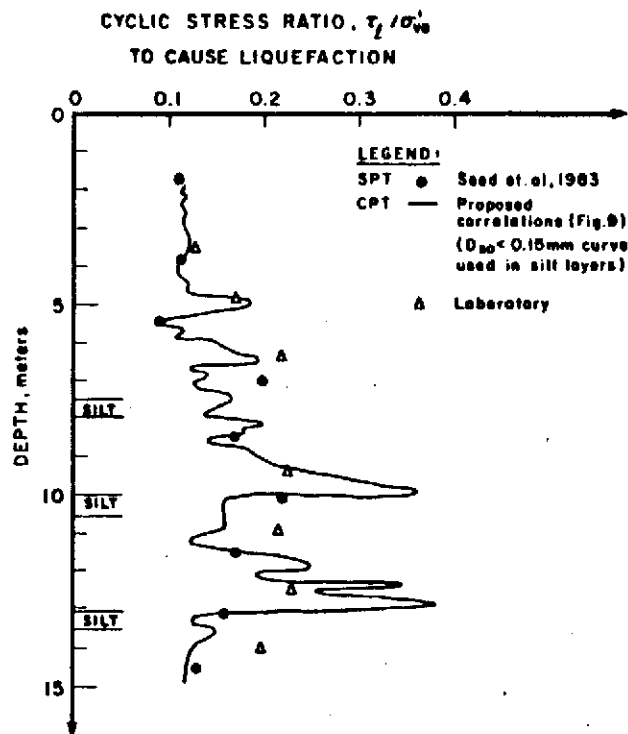


FIG. 14.—Comparison of Predicted Cyclic Stress Ratio to Cause Liquefaction from SPT, CPT and Laboratory Testing at McDonald's Farm Site, B.C.

however, provides a continuous prediction which gives considerable insight into the variation of the cyclic resistance with depth due to the variations in soil conditions.

#### CONCLUSION

Correlations between cyclic stress ratio to cause liquefaction and modified cone bearing have been proposed for sands and silty sands. The correlations are based on empirical relationships and require considerable field verification. However, the proposed correlations provide a basis from which to evaluate the use of CPT data for assessment of field liquefaction. The proposed CPT-based method should be used in a similar manner to the SPT method proposed by Seed, et al. (23). For any given site with level ground conditions and a given value of maximum ground acceleration, the possibility of liquefaction can be evaluated on an empirical basis with the aid of Figs. 2 and 9. By determining the appropriate values of  $Q_c$  (Fig. 2) for the deposit lower bound values of cyclic stress ratio,  $\tau_1/\sigma'_{v0}$ , to cause liquefaction can be obtained (Fig. 9) and compared with the cyclic stress ratio induced by the design earthquake ( $\tau/\sigma'_{v0}$ ). The CPT soil classification chart (Fig. 8) can be used to provide a preliminary identification of liquefaction-susceptible soils and

subsequently be updated or adjusted as additional relevant data are reported.

The proposed CPT correlations were evaluated using field and laboratory data from Canada, Japan, China and the U.S. The proposed correlation for sand ( $D_{50} \geq 0.25$  mm) appears to represent a good lower bound to the available data. The silty sand curve ( $D_{50} < 0.15$  mm) also represents a reasonable lower bound, but several data points plot considerably higher than the lower bound line.

The CPT correlations presented by Seed, et al. (23), are very similar to those proposed here, provided the  $q_c/N$  ratios of 5 and 4.5 are applied for sands and silty sands, respectively. The proposed correlations presented in this paper represent lower bounds, whereas the correlations by Seed, et al. (23) (using  $q_c/N = 5$  and 4.5), may represent boundaries with an 80–90% confidence level.

Cone penetration in fine-grained soils often takes place under undrained or partially drained conditions and dynamic pore pressures can be generated. The addition of continuous pore pressure measurements during cone penetration has the potential to significantly improve our understanding of CPT data for liquefaction assessment in fine-grained soils. However, the use of dynamic pore pressures during cone penetration, as a measure of liquefaction resistance, is extremely difficult to quantify because of soil permeability and variations in cone design. A comprehensive case history to illustrate the importance of cone design in relation to liquefaction assessment was given by Campanella, et al. (4). It was shown that remarkably different dynamic pore-pressure profiles could be obtained in silts for cones with the pore-pressure element located either on or immediately behind the cone tip. Good correlations were obtained between dynamic pore pressures measured behind the tip and liquefaction resistance. However, considerably more research and field verification is required to quantify and clarify the use of dynamic pore pressures during cone penetration testing for liquefaction assessment. This is an area of intense research.

The proposed CPT correlations (Fig. 9) assume the cone bearing to be ultimate values from thick deposits (i.e., uninfluenced by adjacent soil interfaces). If a soil layer is less than 10 to 20 cone diam in thickness, the cone bearing may not reach its ultimate value within the layer because of the close proximity of the adjacent interfaces (16). However, the pore-pressure response is likely to be less influenced by adjacent layers.

CPT data can provide information to identify potential critical areas where a detailed assessment may be required, which may include sampling or further in-situ testing, or both. This is especially so for some fine-grained soils that can be successfully sampled and tested in the laboratory.

#### ACKNOWLEDGMENTS

The assistance of the Natural Sciences and Engineering Research Council; The Department of Energy, Mines and Resources of Canada; Ertec Western; Fugro B.V.; MacLeod Geotechnical; and the technical staff of the Civil Engineering Department of the University of British Colum-

bia is much appreciated. The assistance and support of Professors Y. P. Vaid and P. M. Byrne is gratefully acknowledged. Special thanks to Carol Lore for her careful typing of the manuscript.

#### APPENDIX.—REFERENCES

1. Arulmioli, K., Aralanandam, K., and Seed, H. B., "A New Method for Evaluating Liquefaction Potential In-Situ," Proceedings of ASCE National Convention, St. Louis, Mo., Session 24, 1981 (preprint 81-544).
2. Baldi, G., Bellotti, R., Ghionna, V., Jamiolkowski, M., and Pasqualini, E., "Cone Resistance of a Dry Medium Sand," Proceedings of the 10th International Conference on Soil Mechanics and Foundation Engineering, Stockholm, Sweden, Vol. 2, 1981, pp. 427-432.
3. Baldi, G., Bellotti, R., Ghionna, V., Jamiolkowski, M., and Pasqualini, E., "Design Parameters for Sands from CPT," Proceedings of the Second European Symposium on Penetration Testing, ESOPT II, Vol. 2, Amsterdam, The Netherlands, 1982, pp. 425-438.
4. Campanella, R. G., Robertson, P. K., and Gillespie, D., "Cone Penetration Testing in Deltaic Soils," Canadian Geotechnical Journal, Vol. 20, No. 1, Feb., 1983, pp. 23-35.
5. Christian, J. T., and Swiger, W. F., "Statistics of Liquefaction and SPT Results," Journal of the Geotechnical Engineering Division, ASCE, Vol. 101, No. GT11, 1975, pp. 1135-1150.
6. Dobry, R., Powell, D. J., Yokel, F. Y., and Ladd, R. S., "Liquefaction Potential of Saturated Sand—The Stiffness Method," Proceedings of the 7th World Conference on Earthquake Engineering, held at Istanbul, Turkey, Vol. 3, Sept., 1980, pp. 25-32.
7. Douglas, B. J., "SPT Blowcount Variability Correlated to the CPT," Proceedings of the 2nd European Symposium on Penetration Testing, ESOPT II, held at Amsterdam, The Netherlands, Vol. 1, 1982, p. 41.
8. Douglas, B. J., and Olsen, R. S., "Soil Classification Using Electric Cone Penetrometer," Proceedings of the ASCE Symposium on Cone Penetration Testing and Experience, Geotechnical Engineering Division, St. Louis, Mo., 1981, pp. 209-227.
9. Douglas, B. J., Olsen, R. S., and Martin, G. R., "Evaluation of the Cone Penetrometer Test for SPT Liquefaction Assessment," Geotechnical Engineering Division, presented at the 1981 ASCE National Convention, held at St. Louis, Mo., Session No. 24.
10. Ishihara, K., and Koga, Y., "Case Studies of Liquefaction in 1964 Niigata Earthquake," Soil and Foundations, Japanese Society of Soil Mechanics and Foundation Engineering, Vol. 21, No. 3, Sept., 1981, pp. 35-52.
11. Ishihara, K., Shimizu, K., and Yamada, Y., "Porewater Pressures Measured in Sand Deposits During an Earthquake," Soil and Foundations, Japanese Society of Soil Mechanics and Foundation Engineering, Vol. 21, No. 4, Dec., 1981, pp. 85-100.
12. Iwasaki, T., Tatsuoka, F., Tokida, K., and Yasuda, S., "A Practical Method for Assessing Soil Liquefaction Potential Based on Case Studies at Various Sites in Japan," Proceedings of the 2nd International Conference on Microzonation for Safer Construction Research and Application, 1978.
13. Kovacs, W. D., and Salomone, L. A., "SPT Hammer Energy Measurements," Journal of the Geotechnical Division, ASCE, Vol. 108, No. GT4, Apr., 1982, pp. 599-620.
14. Kovacs, W. D., Salomone, L. A., and Yokel, F. Y., "Energy Measurements in the Standard Penetration Test," U.S. National Bureau of Standards Building Science Series 135, 1981.
15. Peck, R. B., "Liquefaction Potential: Science versus Practice," Journal of the Geotechnical Division, ASCE, Vol. 105, No. GT3, Mar., 1979.
16. Robertson, P. K., and Campanella, R. G., "Interpretation of Cone Penetration Tests, Part I (Sand)," Canadian Geotechnical Journal, Vol. 20, No. 4, Nov., 1983, pp. 718-733.
17. Robertson, P. K., Campanella, R. G., and Wightman, A., "SPT-CPT Correlations," Journal of Geotechnical Engineering, ASCE, Vol. 109, No. GT11, Nov., 1983, pp. 1449-1459.
18. Schmertmann, J. H., "Predicting the  $q_c/N$  Ratio," Final Report D-636, Engineering and Industrial Experiment Station, Department of Civil Engineering, University of Florida, Gainesville, Fla., 1976.
19. Schmertmann, J. H., "Guidelines for Cone Penetration Test, Performance and Design," Report FHWA-TS-78-209, Federal Highway Administration, Washington, D.C., July, 1978, 145 pp.
20. Seed, H. B., "Evaluation of Soil Liquefaction Effects on Level Ground During Earthquakes," Liquefaction Problems in Geotechnical Engineering, ASCE Preprint 2752, Philadelphia, Pa., 1976.
21. Seed, H. B., and Idriss, I. M., "Simplified Procedure for Evaluating Soil Liquefaction Potential," Journal of the Soil Mechanics and Foundations Division, ASCE, Vol. 97, No. SM9, Sept., 1971.
22. Seed, H. B., and Idriss, I. M., "Evaluation of Liquefaction Potential of Sand Deposits Based on Observations of Performance in Previous Earthquakes," Proceedings of the ASCE National Convention, Geotechnical Engineering Division, St. Louis, Mo., Session No. 24, 1981.
23. Seed, H. B., Idriss, I. M., and Arango, I., "Evaluation of Liquefaction Potential Using Field Performance Data," Journal of Geotechnical Engineering, ASCE, Vol. 109, No. 3, Mar., 1983, pp. 458-482.
24. "Standard Method for Deep Quasi-Static, Cone and Friction-Cone Penetration Tests of Soil," ASTM Designation D3441, American Society for Testing and Materials, 1979.
25. Vaid, Y. P., Byrne, P. M., and Hughes, J. M. O., "Dilation Angle and Liquefaction Potential," Journal of the Geotechnical Division, ASCE, Vol. 107, No. GT7, July, 1981.
26. Youd, T. L., and Bennett, M. J., "Liquefaction Sites, Imperial Valley, California," Journal of Geotechnical Engineering, ASCE, Vol. 109, No. 3, Mar., 1983, pp. 440-457.
27. Zhou, S., "Evaluation of the Liquefaction of Sand by Static Cone Penetration Test," Proceedings of the 7th World Conference on Earthquake Engineering, Vol. 3, held at Istanbul, Turkey, 1980.
28. Zhou, S. G., "Influence of Fines on Evaluating Liquefaction of Sand by CPT," Proceedings of the 1981 International Conference on Recent Advances in Geotechnical Earthquake Engineering and Soil Dynamics, held at St. Louis, Mo., Vol. 1, 1981, pp. 167-172.